Dalton Transactions

Covalent and ionic bonding in bi- and tricyclic Group 15 amides: equidistant P–I and As–I bonds and fluxional cations

Journal:	*Dalton Transactions*
Manuscript ID	DT-ART-03-2020-001163.R1
Article Type:	Paper
Date Submitted by the Author:	18-Apr-2020
Complete List of Authors:	Musongong, Joseph; University of North Dakota, Department of Chemistry Otang, Mathew; University of North Dakota, Department of Chemistry Mash, Brandon; Purdue University, Chemistry Zeller, Matthias; Purdue University, Department of Chemistry Stahl, Lothar; University of North Dakota, Department of Chemistry; University of North Dakota

Revised

Covalent and ionic bonding in bi- and tricyclic Group 15 amides: equidistant P–I and As–I bonds and fluxional cations

Joseph T. Musongong,[a] Mathew E. Otang,[a] Brandon L. Mash,[b] Matthias Zeller,[b] and Lothar Stahl*,[a]

[a] Department of Chemistry, University of North Dakota, Grand Forks, ND USA 58202

[b] Department of Chemistry, Purdue University, West Lafayette, IN USA 47907

E-mail: lothar.stahl@und.edu

Phone: 1-701-777-2242

Fax: 1-701-777-2331

Introduction

The study of inorganic-ring systems—once a relatively small domain of non-metal chemistry—has entered the main stream of inorganic chemistry.[1–8] It was the realization that these molecules are more than just structural curiosities that led to their widespread acceptance. Thus, for example, inorganic heterocycles have been used as ligands or as platforms for ligands in main-group and coordination chemistry, [9–29] as building blocks for polymers, [30, 31] macrocycles, [32–36] materials precursors, [37–43] and theory-supported chemical transformations.[44, 45] The extensive amount of work reported in this area in the recent past has been summarized in various reviews. [46–50]

We are investigating the chemistry of four-membered phosphorus-nitrogen rings that are substituted with just enough organic groups to solubilize them in organic solvents. Such compounds have a strong tendency to form polycycles and cages with bond angles close to 90 degrees. A ligand suitable for the creation of such molecules is the bis(*tert*-butylamino)cyclodiphosph(III)azane $\mathbf{LH_2}$ (Chart 1) which when deprotonated with strong bases yields a dianion, $\mathbf{L^{2-}}$, that can encapsulate diverse elements. Consequently, we and others have incorporated metals, metalloids, and nonmetals from across the periodic table into this ligand.

The general utility of **L** as a ligand had been demonstrated by its Group 15 derivatives, shown in Chart 1. These range from the small non-metal phosphorus to the large metal bismuth and thus are a good test of a ligand's versatility. The incorporation of trivalent Group 15 element chlorides afford compounds of structure types **A** and **B**, the exact conformation depending on the nature of the chelated atom. Thus, in heterocycles of type **A** the Group 15 element is centered above the $(PN)_2$ ring in a κ^2*N* mode and three-coordinate, while in type **B** the chelated atom rests above one of the ring nitrogen atoms in a κ^3*N* fashion and has coordination number four.

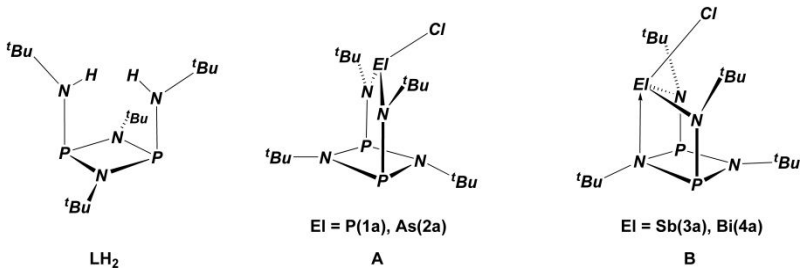

Chart 1. LH_2 and its bicyclic (**A**) and tricyclic (**B**) Group 15 derivatives.

The compounds discussed below all share the bis(*tert*-butylamido)cyclodiphosphazane framework, but differ in the central Group 15 element **El** and its monodentate ligand. One of these compounds, the antimony chloride analog, had previously been synthesized in a serendipitous manner,[6] a fact that affirms the robustness of the structural motif. The chlorides of the bicycles shown in Chart 2, are ideal starting points for the derivatization of these compounds, because chloride can be replaced with a variety of monoanionic ligands, ranging in size from iodide to hexamethyldisilylamide.

We had previously described some of these derivatives and noted that while the reactions seemed straightforward, the products showed rather unusual bond elongations between the central **LEl** moiety and the monodentate ligand **X**.[21, 24] Specifically, it appeared that some of these bonds were significantly longer than the sum of the covalent radii. The presence of a chemical bond is usually invoked when the distance between two atoms is shorter than the sum of their van der Waals radii. While the detection of a bond is straightforward in simple ionic and small covalent compounds, larger molecules often present challenges. Even more complex is the distinction between polar covalent and ionic bonds. At what point is there still a sharing of an electron pair, as in a polar covalent bond, and when is the bond strictly an electrostatic attraction between two ions?

Here we report on the continuation of previous work on Group 15 elements of bis(*tert*-butylamido)cyclodiphosphazanes by chloride substitution. These results will show that the **El–X** interaction can be modified from covalent, via highly polar-covalent to completely ionic, depending on

the nature of the chelated Group 15 element and the monodentate ligand X. To facilitate the discussion we will use the following labels for these compounds. The unique Group 15 atom, **El**, will be labeled with a number, ranging from **1** = P to **4** = Bi, while the ligand **X** will be designated with a small letter, as shown in Chart 3. For example, **2c** denotes the arsenic azide derivative.

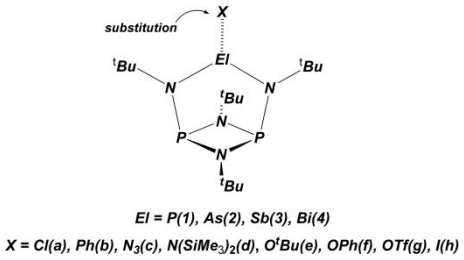

El = P(1), As(2), Sb(3), Bi(4)

X = Cl(a), Ph(b), N_3(c), $N(SiMe_3)_2$(d), O^tBu(e), OPh(f), OTf(g), I(h)

Chart 2. Common structure and alphanumeric labeling scheme for compounds presented in this paper.

Ideally derivatives of all four Group 15 elements with the same mono-dentate ligand should have been synthesized and studied. Unfortunately, this was not possible for two reasons. Firstly, some of these compounds had already been reported earlier by others and us, and secondly, it was not always possible to cleanly synthesize and/or isolate the desired derivative of a given Group 15 element. The compounds described below constitute those compounds that had not been reported before and that were of sufficient purity to be fully characterized.

Results and Discussions

Covalent Compounds

In previous studies on the reaction chemistry of **1a** and its Group 15 homologs, we had substituted chloride with *N*- and *O*-centered monodentate ligands, like azide, hexamethyldisilylamide, and phenoxide.[21,24] But no compounds having carbon-donor ligands were reported. Because of the commercial availability of $PhPCl_2$, we considered the interaction of this dichloride with **$(Li{\cdot}THF)_2L$**,

Scheme 1, the most direct route to the phenylphosphine derivative of **L**. Such a molecule, we thought, might be a new version of a diamino(phenyl)phosphine with potential uses as a ligand.

To our surprise, the reaction did not yield the targeted phenylphosphino-bis(*tert*-butylamino)cyclodiphosphazane **1b**, but afforded two products, namely the bis(phosphine) **(1ab)$_2$** and the diphosphine **(1b)$_2$** in a 3:1 ratio. The latter one of these had previously been isolated by Nöth *et al*. via an unusual reaction sequence.[8] The major product, **(1ab)$_2$**, which is obtained as the sole product when two equivalents of the chlorophosphine are used, can be converted to the minor product, **(1b)$_2$**, by reduction with magnesium powder. A colorless crystal of **(1ab)$_2$** was subjected to a single-crystal X-ray analysis. Detailed crystallographic data of this and all other single-crystal analyses discussed herein appear in their respective CIFs, which are available from the CCDC.

In the bis(phosphine) **(1ab)$_2$** (Fig. 1) each *tert*-butylamido post is attached to one chloro(phenyl)phosphine moiety instead of both amides chelating one phenylphosphine moiety. We had earlier reported an analogous bis(dichlorophosphino)-substituted bis(amido)cyclodiphosph(III)azane,[25] but in that compound the amido groups bore the less bulky cyclohexyl groups. Phosphorus trichloride, by contrast, had reacted with **(Li·THF)$_2$L** to afford the targeted chelated chlorophosphine **1a** cleanly. These observations suggest that the outcome of these reactions is highly dependent on stoichiometry and the steric demands of the electrophiles.

It is apparent that both extraannular phosphorus atoms of **(1ab)$_2$** are chiral and that they are both *S* configured. Because the compound crystallizes in the acentric space group $P2_1$ the crystal must be enantiopure. The crystals are thus the product of a spontaneous resolution. Undoubtedly, the reaction also produced the *R*, *R* enantiomer of the molecule shown in Fig. 1, and very likely in the same amount. Purely by chance, the crystal chosen for the X-ray study was that of the *S*, *S* enantiomer.

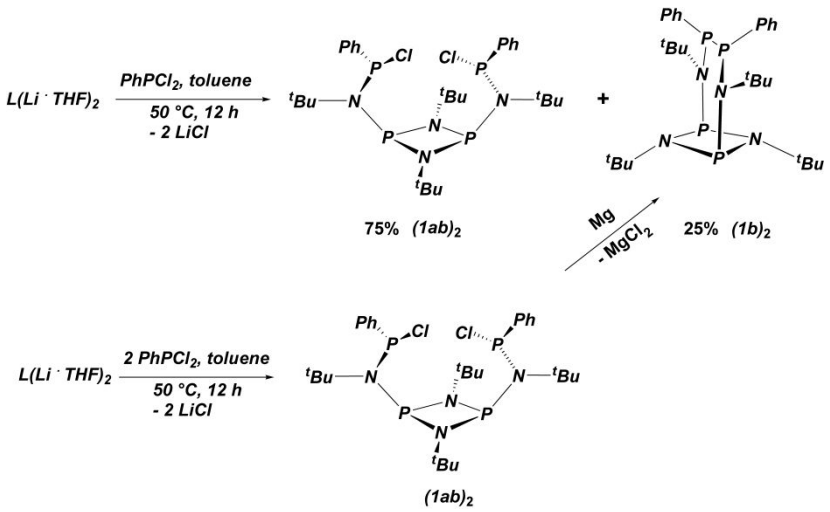

Scheme 1: Syntheses of **(1ab)$_2$** and **(1b)$_2$**

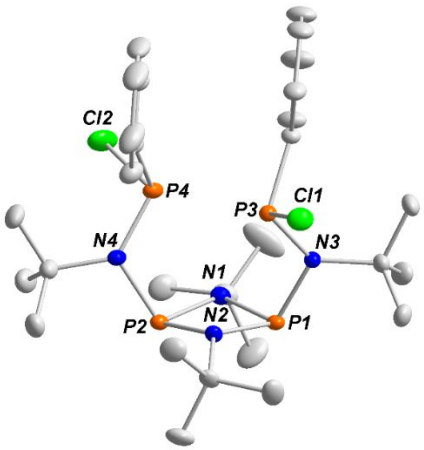

Fig. 1. Solid-state structure and partial labelling scheme of C_2-symmetric (**1ab)$_2$**. Hydrogen atoms have been omitted, and all atoms are drawn at the 50% probability level. Selected bond lengths (Å) and angles (°): P3–N3 1.6868(17), P3–Cl1 2.1135 (7), P3–C1 1.835 (2), P4–N4 1.6967(18), P4–Cl2 2.1474(8), P4–C51 1.844 (2), P1–N3 1.7519(17), P2–N4 1.7636(17), P1–N1 1.7347(17), P1–N2 1.7202(16), P2–N1 1.7134(17), P2–N2 1.7327(17); N3–P3–Cl1 101.00(9), N3–P3–C1 107.20(8), Cl1–P3–C1 99.35(7), N4–P4–Cl2 105.27(4), N4–P4–C51 107.49(10), Cl2–P4–C51 98.47(7).

The amino-, chloro-, phenyl-substituted phosphorus atoms P3 and P4 of **(1ab)$_2$** feature the typical pyramidal structure associated with tertiary phosphines, having P–C, P–N, and P–Cl bonds of ordinary lengths. Expectedly, the bond angles about both phosphorus atoms, vary widely from 98.47(7) to 107.49(10) degrees.

Because of our failure to synthesize the targeted phenylphosphine derivative from **(Li·THF)$_2$L** and $PhPCl_2$, we resorted to treating **1a** with a phenylmagnesium chloride solution, as this is also the only efficient route to the arsenic and antimony analogs. The substitution of chloride in **1a**, **2a**, and **3a** with a phenyl ring, Scheme 2, proceeded readily at room temperature.

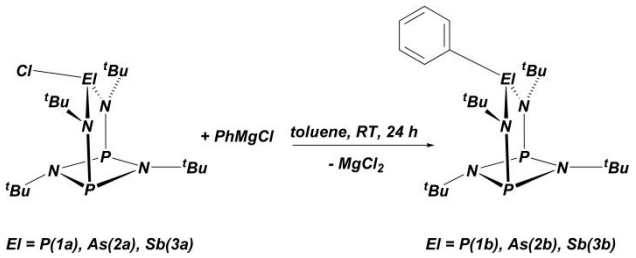

Scheme 2. Syntheses of the phenyl derivatives **1b**, **2b**, and **3b**.

The three homologs were isolated in almost quantitative yields as colorless crystals, but only those of arsenic (**2b**) and antimony (**3b**) were suitable for single-crystal X-ray analysis. Fig. 2 shows that the arsenic atom of **2b** is perfectly centered above the $(PN)_2$ heterocycle, being chelated by two symmetric As–N bonds of normal-lengths. In this bicycle the arsenic atom, which forms a 1.981(3) Å long bond with the phenyl group, tops a trigonal pyramid with an angle sum of 302.24°.

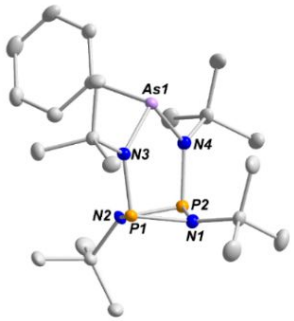

Fig. 2. Solid-state structure and partial labelling scheme of **2b**. Hydrogen atoms have been omitted, and all atoms are drawn at the 50% probability level. Selected bond lengths (Å) and angles (°): As1–N3 1.899 (2), As1–N4 1.908(2), As1–C1 1.981(3), P1–N3 1.695(2), P2–N4 1.697(2), P1–N1 1.722(2), P1–N2 1.736(2), P2–N1 1.725(2), P2–N2 1.746(2); N3–As1–N4 101.00(9), N3–As1–C1 101.37(10), N4–As1–C1 99.87(10), N1–P1–N2 82.86(11), N1–P2–N2 82.48(11).

The antimony derivative **2b**, Fig. 2, is of type **B**, but otherwise entirely structurally analogous to that of its arsenic counterpart. The Sb–N bonds have normal lengths, although the Sb1…N1 donor bond is elongated (2.774(5) Å) compared to that in the chloride precursor (2.3972(13) Å), possibly reflecting a decreased Lewis acidity in the metalloid due to the substitution of chloride by phenyl. Expectedly, the trigonal pyramid formed by Sb1, N3, N4, and C1, having an angle sum of only 292.56°, is even more pointed here than in **2b**.

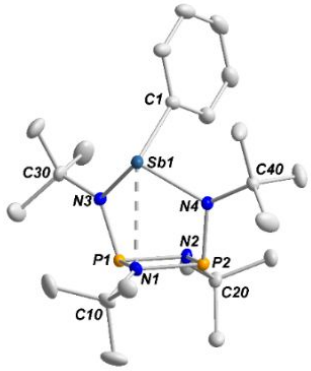

Fig. 3. Solid-state structure and partial labelling scheme of **3b**. Hydrogen atoms have been omitted, and all atoms are drawn at the 50% probability level. Selected bond lengths (Å) and angles (°): Sb1–N1 2.7437(10), Sb1–N3 2.1113(10), Sb1–N4 2.1057(10), Sb1–C1 2.1635(12), P1–N3 1.6682(10), P2–N4

1.6734(10), P1–N1 1.7371(9), P1–N2 1.7395(10), P2–N1 1.7416(10), P2–N2 1.7390(9); N3–Sb1–N4 105.04(4), N3–Sb1–C1 94.01(4), N4–Sb1–C1 93.51(4), N1–P1–N2 82.06(5), N1–P2–N2 81.95(5).

The ^{1}H NMR spectra of **1b, 2b, 3b** confirm that the solution structures are analogs of the solid-state structures, as all compounds show a configurationally locked phenyl ring that hovers over one of the *tert*-butylimido groups. This creates three sets of chemically- and magnetically-different *tert*-butyl groups, which in turn leads to three ^{1}H NMR signals that are present in a 1:2:1 ratio. While **1b** exhibits two phosphorus signals at 203.1 (d) and 69.7 (s), the ^{31}P{^{1}H} NMR spectra of **2b** and **3b** expectedly showed only one singlet each at 172.1 and 138.3 ppm, respectively.

The *tert*-butoxy, respectively phenoxy, derivatives **1e**, **3e**, and **2f** (Scheme 3) were obtained by treatment of the Group 15 element chlorides with sodium *tert*-butoxide and sodium phenoxide, respectively. Although **1e** and **3e** furnished well-shaped colorless crystals, extensive disorder in the crystals of both compounds prevented even the solution of their crystal structures. The ^{1}H, ^{13}C{^{1}H}, and ^{31}P{^{1}H} NMR data, however, leave little doubt that **1e** and **3e** have the structures shown in Scheme 3.

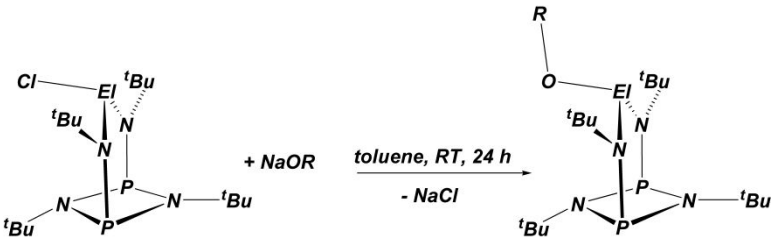

Scheme 3. Syntheses of **1e, 3e**, and **2f**

Hexamethyldisilylamide (HMDS) is a large monodentate N-donor ligand that is typically chosen when low-coordination is desired. Despite the bulk of this ligand and the steric congestion of bismuth in **4a**, the reaction shown in Scheme 4 afforded colorless **4d** cleanly and in a 78% yield. The somewhat reduced yield may be due to the greater solubility of this compound in toluene.

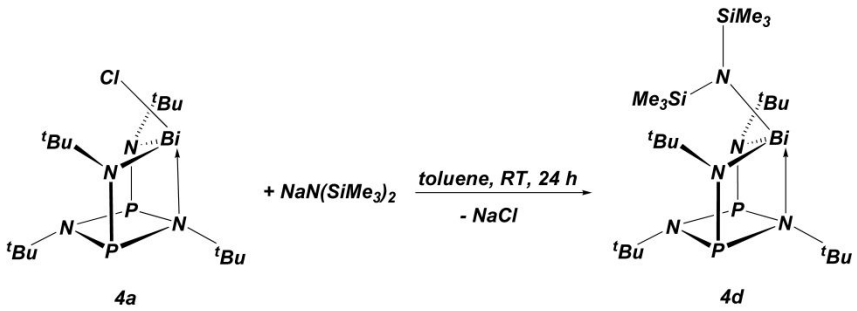

Scheme 4: Synthesis of **4d**

Figure 4 shows the solid state structure of **4d**, which expectedly adopted structure type **B**. The metal atom forms three equidistant covalent Bi–N bonds of ca. 2.26 Å lengths to the chelating ligand and the monodentate HMDS, all nitrogen atoms being sp^2 hybridized. Unsurprising is the longer donor bond (2.733(3) Å) from the basal nitrogen atom.

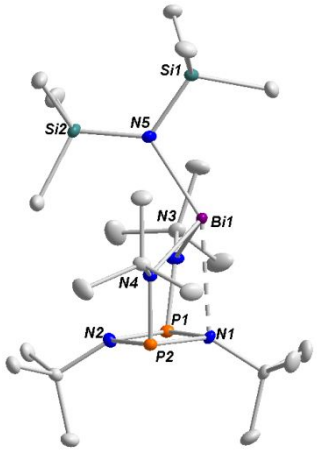

Fig. 4. Solid-state structure and partial labelling scheme of **4d**. Hydrogen atoms have been omitted and all atoms are drawn at the 50% probability level. Selected bond lengths (Å) and angles (°): Bi1–N1 2.733(2), Bi1–N3 2.222(2), Bi1–N4 2.236(2), Bi1–N5 2.217(2), P1–N3 1.682(2), P2–N4 1.675(2), P1–N1 1.757(2), P1–N2 1.735(2), P2–N1 1.759(2), P2–N2 1.730(2); N3–Bi1–N4 98.90(8), N3–Bi1–N5 101.09(8), N4–Bi1–N5 101.88(8), N1–P1–N2 82.86(11), N1–P2–N2 82.48(10).

While also a nitrogen donor, the pseudohalide azide is not only substantially smaller than HMDS it also features a more delocalized negative charge. The arsenic azide derivative **2c** was obtained by the

straightforward treatment of **2a** with one equivalent of sodium azide in room-temperature toluene, as shown in Scheme 5. NMR data immediately identified the product as an analog of $CPTPN_3$[24] and $CPTSbN_3$.[21] The structure of **2c**, Fig. 5, which is of type **A** has mirror symmetry, the mirror plane including the arsenic atom, the azide ligand, and the nitrogen atoms of the four-membered ring. The $(PN)_2$ ring is noticeably buckled, and the *tert*-butyl substituent of N2 is pushed significantly below the cyclodiphosphazane plane due to its repulsive interaction with the azide moiety.

Although the solid-state structure of **2c** is similar to those of its congeners, the azide ligand displays a different conformation from those in $CPTPN_3$ and $CPTSbN_3$ by pointing towards the $(PN)_2$ ring, rather than upwards.

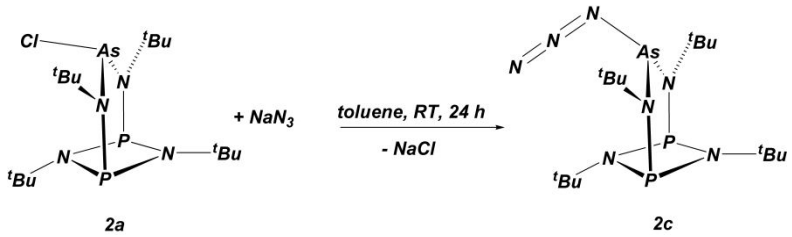

2a 2c

Scheme 5: Synthesis of **2c**

The $As–N_3$ bond, which is substantially longer at 1.9668(17) Å than the symmetric As–N(amide) bonds (1.8505(9) Å), is also significantly longer than the $As–N_3$ bond in homoleptic $As(N_3)_3$,[51, 52] where the As–N bonds have an average length of ca. 1.90 Å. The long As–azide bond in **2c** seems to suggest ionic bonding, and this hypothesis is further supported by the nitrogen–nitrogen bonds within the azide moiety. These are almost isometric with N4–N5 = 1.175(2) Å and N5–N6 = 1.157(3) Å and are thus quite similar in length to those of alkali-metal azides.[53] Group 15 element azide compounds typically show one long, and one short nitrogen-nitrogen bond, as is expected for covalent azides.[54, 55]

Polar-Covalent Compounds

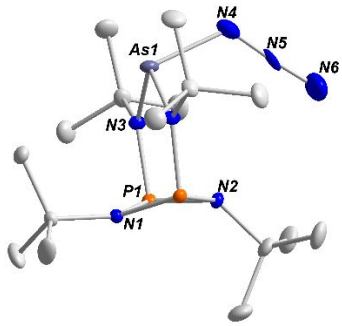

Fig. 5. Solid-state structure and partial labelling scheme of **2c**. Hydrogen atoms have been omitted, and all atoms are drawn at the 50% probability level. Selected bond lengths (Å) and angles (°): As1–N3 1.8505(9), As1–N4 1.9668(17), P1–N1 1.7180(9), P1–N2 1.7393(9), P1–N3 1.7154(9), N4–N5 1.175(2), N5–N6 1.157(3); N3–As1–N3' 101.00(9), N3–As1–C1 101.75(6), N3–As1–N4 102.02(4), N1–P1–N2 83.26(5), P1–N1–P1' 95.69(6), P1–N2–P1' 95.69(6) .

The unusual bonding in the arsenic azide **2c** prompted us to re-evaluate the pnictogen-halogen interactions in these compounds. Previous structural studies by Scherer *et al*.[6] and us had shown elongated El–Cl bonds, and we expected this effect to be more pronounced in phosphorus-iodide bonds. But while the triiodides of arsenic and antimony are well behaved compounds, the phosphorus analog is significantly less stable and not a convenient source for iodophosphines. To synthesize the iodide analogs of **1a**, **2a** and **3a**, we treated these chlorides with NaI, as shown in Scheme 5. All reactions proceeded surprisingly fast at room temperature and were complete within 24 hours.

The ^{1}H NMR spectra, however, revealed only two, rather than the expected three singlets for the *tert*-butyl groups, both *tert*-butylimido groups appearing as one broad signal. This lack of configurational stability suggests that the element-iodide bond either swings from side to side, or that the iodide ion, if indeed it is an ion, moves over the bicyclic cation, from one side to the other, thereby rendering both *tert*-butylimido groups equivalent.

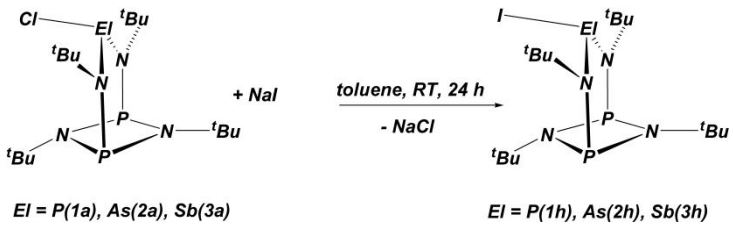

Scheme 6. Syntheses of **1h**, **2h**, and **3h**.

All three iodides were isolated as light-yellow crystals and subjected to single crystal X-ray analyses. Figures 6 and 7 show the solid-state structures of **1h** and **2h** respectively. These mirror-symmetric compounds are of structure type **A**, the phosphorus and arsenic atoms being located centrally above the $(PN)_2$ ring. The element amide bonds (P–N3 = 1.6783(10) Å and As–N3 = 1.8364(10) Å) differ by 0.1582(7) Å and thus reflect reasonably well the difference in the covalent radii of phosphorus and arsenic (0.14 Å).[56] One would expect a similar difference in the lengths of phosphorus–iodide and arsenic–iodide bonds. As measured in these crystals, however, the P–I and As–I bonds are almost isometric at 2.7340(5) and 2.7373(3) Å, respectively. Based on the covalent radii of these three elements bonds lengths of ca. 2.39 and 2.53 Å, respectively, would be expected, and such bond lengths have been reported for related phosphorus-iodine bonds.[57, 58] The bond lengths observed in **1h** and **2h** are thus not only significantly longer than they should be, and by 0.34 and 0.20 Å, respectively, but they are also equidistant! This seems to suggest that in **1h** and **2h** the central Group 15 element and the iodine atoms do not form covalent bonds. Rather, the iodide ions are electrostatically attracted by the phosphenium,[59–62] respectively arsenium, ions. Because the phosphorus atom is buried deeper in the bulk of the bicycle than arsenic, its bond to iodide is more elongated.

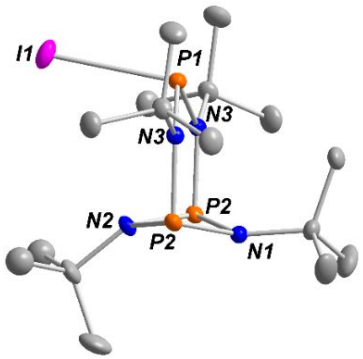

Fig. 6 Solid-state structure and partial labelling scheme of **1h**. Hydrogen atoms have been omitted, and all atoms are drawn at the 50% probability level. Selected bond lengths (Å) and angles (°): P1–I1 2.7340(5), P1–N3 1.6788(8), P2–N1 1.7188(8), P2–N2 1.7164(8), P2–N3 1.7525(8); N3–P1–N3' 104.64(5), N3–P1–I1 102.67(3), N1–P2–N2 83.24(4), P2–N1–P2' 94.46(6), P2–N2–P2' 94.64(6).

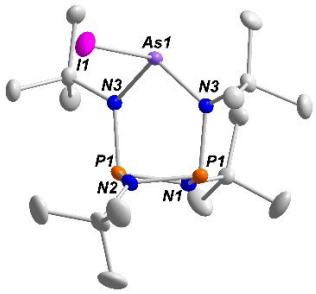

Fig. 7 Solid-state structure and partial labelling scheme of **2h**. Hydrogen atoms have been omitted, and all atoms are drawn at the 50% probability level. Selected bond lengths (Å) and angles (°): As1–I1 2.7373(3), As1–N3 1.8364(10), P1–N1 1.7187(10), P1–N2 1.7242(10), P1–N3 1.7273(11); N3–As1–N3' 102.41(6), N3–As1–I1 102.03(3), N1–P1–N2 82.86(5), P1–N1–P1' 95.71(7), P1–N2–P1' 95.31(7).

To gain further insight into the unusual bond lengthening in these iodides, we also scrutinized the Sb–I bond in **3h**, a compound which is of structure type **B**. Like **1h** and **2h,** the antimony analog is also mirror symmetric, albeit not in a crystallographic sense. Both Sb–N bonds are 2.10 Å long, and thus

slightly shorter than the sum of the covalent radii of Sb and N, the shortening again likely being due to the sp^2 hybridization of the nitrogen atoms. Here too, however, the Sb–I bond (2.9100(3) Å) is ca. 0.18 Å longer than the sum of the covalent radii of the metalloid and the halogen. Because the absolute bond lengthening is smallest for the largest pnictogen, the assumption that steric hindrance of the central pnictogen is the major factor in the bond lengthening seems reasonable.

While the claim of iconicity in the azides of the title compounds is somewhat circumstantial and rests mostly on a slightly elongated As–N bond and symmetric N–N bonds, the Group 15 element iodide bonds are clearly substantially longer than those in covalent iodides[57, 58] and appear to be the result of ion-pair formation. This claim is also supported by the unusually high melting point of **1h**, which is ca. 60 °C higher than that of its chloride analog.

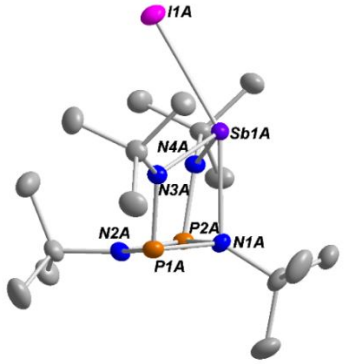

Fig. 8 Solid-state structure and partial labelling scheme of one of the two independent molecules of **3h**. Hydrogen atoms have been omitted, and all atoms are drawn at the 50% probability level. Selected bond lengths (Å) and angles (°): Sb1A–I1A 2.9100(3), Sb1A–N3A 2.102(2), Sb1A–N4A 2.094(2), Sb1A–N1A 2.420(2), P1A–N3A 1.685(2), P2A–N4A 1.682(2), P1A–N1A 1.781(2), P1A–N2A 1.721(2), P2A–N1A 1.775(2), P2A–N2A 1.715(2); N3A–Sb1A–N4A 104.01(9), N3A–Sb1A–I1A 95.65(6), N4A–Sb1A–I1A 96.72(7), N1A–P1A–N2A 80.54(11), N1A–P2A–N2A 80.88(12).

Ionic Compounds

The substitutions described to this point were all conventional salt elimination reactions which yielded covalent compounds via a presumed S_N2 mechanism. The structure of **1h**, however, had already indicated that this iodide could be considered partly ionic, because the P–I bond is more than 14% longer than the sum of the covalent radii of phosphorus and iodine.

The chloride ligand may be displaced without substitution if suitable, non-coordinating ligands are introduced. This, we expected, would reveal the full ionic character of the bi-, respectively tricycle. Thus, treatment of **1a** with one equivalent of silver(I) triflate, Scheme 7, did not yield a substitution product, but furnished a salt, **1g**, consisting of a cationic tricyclic phosphorus species (a phosphonium ion) and a non-coordinating triflate ion.

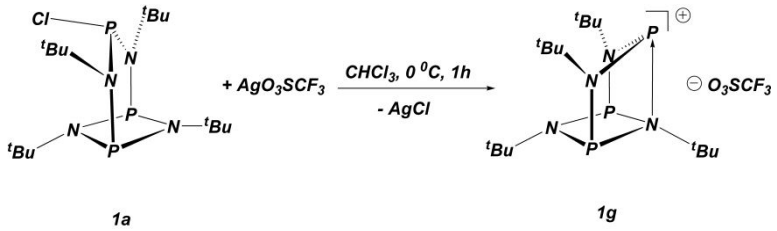

1a *1g*

Scheme 7. Synthesis of **1g**.

The structure of the cation of **1g** with a partial atom numbering scheme is shown in Fig. 9, while selected bond parameters are given in the figure caption. The colorless salt crystallizes in the cubic space group $P2_13$, with four formula units per unit cell. Here the tricyclic cation and the triflate ion are clearly an ion pair, because the shortest contact between any oxygen atom of the triflate ion and the phosphorus atom of the cation is 5.881 Å. It is also possible to view the cation as an internally-stabilized phosphenium ion.[59–62]

Both, the cation and anion, lie on crystallographic threefold rotation axes, but while the anion satisfies the site symmetry, the cation does not and is therefore disordered. The cation is a seco-

heterocube, i. e., a cube with one missing corner. The crystallographic axis, which is a pseudo body-diagonal of the *seco*-cube passes through P1 and approximately through C20, the quaternary carbon atom to which N2 is attached. Because N2 does not lie on the axis, it and its attached *tert*-butyl group (C20) are disordered. Only one of the three images of N2 and the *tert*-butyl group are shown. The threefold axis also generates three P2 atoms, while only two off-axis phosphorus atoms (P2) are present. The view in Fig. 9 is approximately along the line of the "missing phosphorus" atom.

Because of the disorder, the phosphorus-nitrogen bond lengths of the *seco*-heterocube are afflicted with relatively high uncertainties. The three crystallographically unique phosphorus-nitrogen bonds, namely P1–N1 = 1.750(5) Å, P2–N1 = 1.816(5) Å, and P2–N2 = 1.728(11) Å, are all comparatively long and fall into two groups, the bonds to P2 being substantially longer.

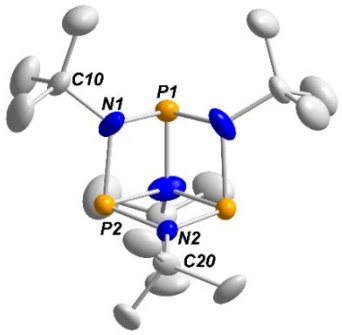

Fig. 9. Solid-state structure and partial labelling scheme for the cation of **1g**. All atoms are drawn at the 50% probability level. Selected bond lengths (Å) and angles (°):P1–N1 1.750(5), P2–N1 1.816(5), P2–N2 1.728(11); P1 N1 P2 96.2(2), P2 N2 P2' 95.3(3).

The solution-phase NMR spectra of **1g**, however, are those of a much more symmetrical molecule than that shown in Fig. 9. Thus, only one singlet was observed in the $^{31}P\{^{1}H\}$ NMR spectrum, while two signals in a 2:1 ratio are expected. The ^{1}H NMR spectrum of the molecule shown in Fig. 9 should exhibit a 1:2:1 pattern of signals but only two singlets, present in a 3:1 ratio, were observed. In solution the cation likely has the C_{3v}-symmetric structure shown in Chart 4. In this structure all three

phosphorus atoms are equivalent as are three of the *tert*-butyl groups, while the axial *tert*-butyl group is unique. Upon cooling to –90 °C no changes in the $^{31}P\{^{1}H\}$ and ^{1}H NMR spectra of **1g** were observed, suggesting that the activation energies for the molecular rearrangement must be very low indeed.

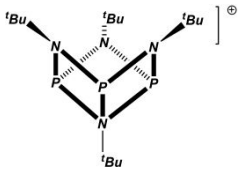

Chart 4. Proposed C_{3v}-symmetric solution structure for the cation of **1g**

Strong support for the proposed solution structure is provided by the coupling patterns. The primary carbon atoms of the unique *tert*-butyl group appear as a quartet, due to their coupling to the three equivalent phosphorus atoms. The primary carbon atoms of the three *tert*-butyl groups at the rim of the funnel-shaped ion are triplets, each being split by two equivalent phosphorus atoms. It is important to remember that the threefold axis in solution (Chart 4) is not identical with the crystallographic threefold axis.

Believing that the triflate ion was key to the generation of ionic compounds, we attempted to replicate **1g** in an antimony analog and treated **3a** with silver(I) triflate (Scheme 8). A similar chloride abstraction as in Scheme 7 occurred, but the ^{1}H NMR spectrum showed only two singlets of equal intensity, consistent with a time-averaged C_{2v}-symmetric structure. Here too cooling of the sample to -80 °C failed to freeze out the ground state of the solid-state structure shown in Fig. 10.

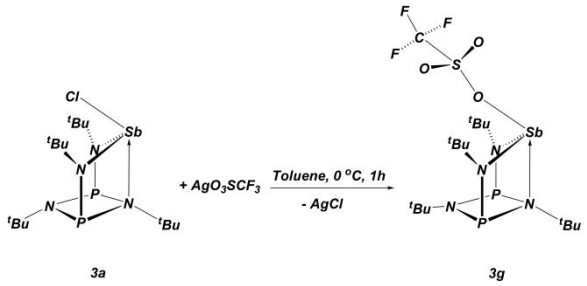

Scheme 8. Synthesis of **3g**.

The colorless crystals obtained from the reaction were subjected to a single-crystal X-ray analysis, the results of which may be seen in Fig. 10. Unlike **1g**, the antimony analog is a covalent compound of structure type **B** in the solid state. Its Sb1–O3 bond is 2.3652(14) Å long, and thus ca. 0.22 Å longer than the sum of the covalent radii of these elements, but it is also substantially longer than the Sb–O bond of 2.158(1) Å in $[(Me_3Si)_2N]_2SbOTf$, reported by Schulz et al.[63] This long bond reflects a very weak, and presumably ionic, antimony–triflate interaction. A charged antimony center is also suggested by the very short N to Sb donor bond of only 2.3029(14) Å—the by far shortest bond of its kind in antimony complexes of **L**, which range from 2.420(2) Å in **3b** to 2.7437(10) Å in **3h**.

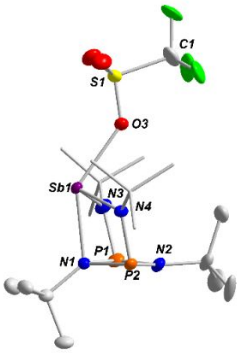

Fig. 10. Solid-state structure and partial labelling scheme of **3g**. With the exception of carbon (35%) all atoms are drawn at the 50% probability level. *Tert*-butylamido carbon groups are drawn as sticks for visual clarity. Selected bond lengths (Å) and angles (°): Sb1–O3 2.3651(15), Sb1–N1 2.3030(14), Sb1–N3 2.0610(17), Sb1–N4 2.0662(15), P2–N4 1.6825(17), P1–N1 1.7970(17), P1–N2 1.717(2), P2–N1

1.8008(17), P2–N2 1.717(2), S1–O1 1.436(2), S1–O2 1.4371(19), S1–O3 1.4701(15), C–F(avg.) 1.321(5), S1–C1 1.822(3); N3–Sb1–N4 104.30(7), N3–Sb1–O3 87.14(7), N4–Sb1–O3 87.00(6).

Given that **1g** exists as an ion pair, the presence of the Sb-triflate bond is a surprise, but it can be rationalized, both sterically and electronically. In this antimony analog the positive charge is localized on the metalloid, rather than being delocalized over the entire tricycle, as it is in **1g**. Antimony is also larger than phosphorus and thus more accessible to the triflate ion. Both factors favor a covalent bond, as it exists in the solid state. But it is a very weak bond that appears to fall apart in solution, as the ^{13}C chemical shifts of the triflate ion in **1g** and **3g** are identical.

Because our interest in these compounds lay in the chelating portion of the bis(*tert*-butylamido)cyclodiphosph(III)azane ligand, we made no mention of the bond parameters of the $(PN)_2$ heterocycle and its *tert*-butylimido substituents. A few general observations regarding these are worth mentioning. Distortions of the heterocycle and it substituents are caused by three factors: a) bond strain within the N–El–N chelate moiety, due to the fit or misfit of the central Group 15 element, b) steric repulsion of *tert*-butylimido groups by the mono-dentate ligand, and c) steric repulsion of the *tert*-butylimido group by Sb and Bi atoms in compounds of structure type **B**. The Group 15 elements phosphorus and arsenic are too small for the chelation gap, resulting in a noticeable buckling of the $(PN)_2$ ring along the N…N line. The larger Group 15 elements antimony and bismuth, by contrast, sterically crowd the *tert*-butyl groups of the imido atoms, causing them to be pushed significantly below the $(PN)_2$ plane. This results in a noticeable pyramidalization of the nitrogen atoms, with bond-angle sums at nitrogen as low as 336 degrees. Similar pyramidalization of the $(PN)_2$ nitrogen atoms are seen when the monodentate ligand sterically repels the *tert*-butylimido group underneath it, as for example in **4d**, where both types of steric repulsion are clearly visible.

Summary and Conclusion

The main goal of this study was to investigate the nature of the bond between the central Group 15 element in bi- and tricyclic amides of the general formula $[(^tBuNP)_2(^tBuN)_2]ElX$, El = P, As, Sb, Bi, and their monodentate ligands X. To a first approximation these compounds may be described as X-ligand-di(*tert*-butylamino)phosphines, -arsines, -stibines, and -bismuthines and their derivatives. But this similarity is deceptive, because the title compounds possess a much narrower coordination gap than that present in their acyclic analogs. Moreover, three lone pairs residing in p orbitals of sp^2-hybridized nitrogen atoms line the inside of this pocket, making access to the chelated Group 15 element difficult. As a result of these steric and electronic constraints, the monodentate ligands exhibited various bonding interactions with the central element, ranging from purely covalent via highly polar to completely ionic.

Strongly nucleophilic C- and N-donors, like phenyl and HMDS, seem to have little difficulty forming good σ-bonds with the central Group 15 element, as long as their steric bulk is peripheral. Resonance-stabilized anions, e. g., azide, and large monoatomic ions, like iodide, by contrast appear to be unable to form proper covalent bonds

Only the triflate ion creates a compound, **1g**, which is truly an ion pair. In solution the cationic phosphorus tricycle, whose positive charge is delocalized over all three phosphorus atoms, exhibits a highly symmetrical funnel shape not previously seen in any other derivative of **L**. The analogous stibonium triflate **3g** does show a very weak covalent bond in the solid state, but it too appears to be fully dissociated into cation and anion in solution.

Alternatively, the bonding variations in these molecules may be interpreted as being due to the ability of these bi- and tri-cyclic cages to delocalize the incipient- or full-fledged positive charge. This makes them weakly-coordinating, and hence selective, cations that bind only strong nucleophiles well.

Experimental section

General procedures

All experimental procedures were performed under an atmosphere of argon, using standard Schlenk techniques. Immediately before use, solvents were dried and freed of dioxygen by distillation under a nitrogen atmosphere from sodium- or potassium benzophenone ketyl. Phosphorus trichloride, *n*-butyllithium (2.5 M in hexanes), and PhMgCl (1.9 M) were purchased from Sigma Millipore or Alfa Aesar and used without further purification. The compounds *cis*–$[(^tBuNP)_2(^tBuNH)_2]$,[1] **L**, *cis*-$[(^tBuNP)_2(^tBuNLi{\cdot}thf)_2]$,[19] $[(^tBuNP)_2(^tBuN)_2]PCl$,[24] **1a**, $[(^tBuNP)_2(^tBuN)_2]AsCl$,[24] **2a**, $[(^tBuNP)_2(^tBuN)_2]SbCl$,[21] **3a**, $[(^tBuNP)_2(^tBuN)_2]BiCl$,[21] **4a**, $[(^tBuNP)_2(^tBuN)_2]PN_3$,[24] **1c**, $[(^tBuNP)_2(^tBuN)_2]PN(SiMe_3)_2$,[24] **1d**, $[(^tBuNP)_2(^tBuN)_2]SbN_3$,[21] **3c**, and $[(^tBuNP)_2(^tBuN)_2]SbN(SiMe_3)_2$,[21] **3d,** were synthesized according to published procedures. All fritted filter tubes used were of medium porosity.

NMR spectra were recorded on a Bruker AVANCE-500 NMR spectrometer. The ^1H and ^{13}C NMR spectra are referenced relative to C_6D_5H (7.15 ppm), CD_2Cl_2 (5.32 ppm), $CDCl_3$ (7.27 ppm), CD_2Cl_2 (53.5 ppm), $CDCl_3$ (77.23 ppm) and C_6D_6 (128.0 ppm), respectively, as internal standards, while the $^{31}P\{^1H\}$ spectra are referenced relative to external $P(OEt)_3$ (137.0 ppm). In all cases positive chemical shift values represent higher frequencies and downfield shifts. Melting points (uncorrected) were recorded on a Mel-Temp melting point apparatus. Elemental analyses were performed by ALS Life Sciences Division Environmental, Tucson, AZ.

Syntheses

$\{[(^tBuNP)_2(^tBuNP)_2](PhCl)_2\}$ $(1ab)_2$

A stirred, cold (0 °C) solution of dichloro(phenyl)phosphine (1.77 g, 9.91 mmol) in toluene (30 mL) was treated dropwise with a solution of **$(Li{\cdot}THF)_2L$** (2.50 g, 4.96 mmol) in THF. A white precipitate formed instantly, and the reaction mixture was allowed to warm to rt and then stirred for 24 h. The precipitate

was removed and the ensuing colorless solution was concentrated *in vacuo* and stored at –12 °C to produce colorless, cubic crystals of **(1ab)$_2$** after 3 days. Yield: (2.85, 4.50 mmol), 91%. Mp: 154–156 °C. ^{1}H NMR (C_6D_6, 25 °C): 7.54 (s, 4H, Ph, *ortho*), 7.01 (m, 4H, Ph, *meta*), 6.96 (m, 2H, Ph, *para*), 1.68 (s, 18H, N^{t}Bu, amido), 1.49 (s, 18H, N^{t}Bu, imido). ^{13}C{^{1}H} NMR (C_6D_6, 25 °C): 141.40 (t, J_{PC} = 28.28 Hz, Ph, *ipso*), 130.64 (t, J_{PC} = 12.28 Hz, Ph, *ortho*), 127.35 (s, Ph, *meta*), 65.17(m, NC(CH$_3$)$_3$, amido), 54.56 (t, J_{PC} = 14.46 Hz, NC(CH$_3$)$_3$, imido), 33.78 (t, J_{PC} = 5.75 Hz, NC(CH$_3$)$_3$, amido), 32.14 (t, J_{PC} = 7.25 Hz, NC(CH$_3$)$_3$, imido). ^{31}P{^{1}H} NMR (C_6D_6, 25 °C): 129.39 (s), 113.75 (s). Anal. Calcd. for $C_{28}H_{46}Cl_2N_4P_4$: C, 53.09; H, 7.32; N, 8.84. Found: C, 53.32; H, 7.30; N, 8.72.

{[(N^{t}BuNP)$_2$(N^{t}BuNP)$_2$]Ph$_2$} (1b)$_2$

A 50 mL flask was charged with **(1ab)$_2$** (0.24 g, 0.38 mmol) and magnesium powder (0.012 g, 0.53 mmol). Tetrahydrofuran (20 mL), was added and the mixture was refluxed for 24 h. Unreacted Mg and $MgCl_2$ were filtered off, and the filtrate was concentrated *in vacuo* and stored at – 12 °C to furnish colorless crystals of **(1b)$_2$** after 24 h. Yield: (0.19 g, 0.34 mmol), 89%. Mp: 210–212 °C. ^{1}H NMR (C_6D_6, 25 °C): 8.08 (m, 4 H, Ph, *ortho*), 7.16 (m, 4H, Ph, *meta*), 7.04 (m, 2H, Ph, *para*), 1.50 (s, 18H, P–P(P)N^{t}Bu), 1.22 (s, 18H, N^{t}Bu, imido). ^{13}C{^{1}H} NMR (C_6D_6, 25 °C): 143.62 (t, J_{PC} = 5.34 Hz, Ph, *ipso*), 131.37 (t, J_{PC} = 16.32 Hz, Ph, *ortho*), 127.76 (s, Ph, *meta*), 127.20 (s, Ph, *para*), 59.62 (m, NC(CH$_3$)$_3$, amido), 55.31 (t, J_{PC} = 20.69 Hz, NC(CH$_3$)$_3$, imido), 33.85 (m, NC(CH$_3$)$_3$, amido), 31.02 (t, J_{PC} = 8.75 Hz, NC(CH$_3$)$_3$, imido). ^{31}P{^{1}H} NMR (C_6D_6, 25 °C): 134.29 (s, P_2N_2), 29.74 (s, P–Ph). (The data are identical with those of a published report.[8])

[(N^{t}BuNP)$_2$(N^{t}BuN)$_2$]PPh, 1b

To a cooled (0 °C) solution of **1a** (0.70 g, 1.7 mmol) in toluene (25 mL) was added dropwise an ethereal solution of PhMgCl (0.87 mL, 1.8 mmol). The mixture was stirred at rt for 24 h and then filtered with a frit. The ensuing light-yellow solution was concentrated *in vacuo* and stored at 12 °C to furnish

colorless plates. Yield: (0.67 g, 1.5 mmol), 88%. Mp: 126–128 °C. ^{1}H NMR (benzene-d_6, 25 °C): 7.82 (td, 2H, *J* = 6.20, 1.75 Hz, Ph), 7.21 (td, 2H, *J* = 7.60, 2.15 Hz, Ph), 7.06 (td, 1H, *J* = 7.30, 1.10 Hz, Ph), 1.62 (s, 18H, N^{t}Bu, amino), 1.29 (s, 9H, N^{t}Bu, imino, N1), 1.00 (s, 9H, N^{t}Bu, imino, N2). ^{13}C{^{1}H} NMR (benzene-d_6, 25 ^{o}C): 152.0 (d, J_{PC} = 21.4 Hz, Ph, *ipso*), 129.3 (d, J_{PC} = 19.2 Hz, Ph), 126.5 (d, J_{PC} = 1.86 Hz, Ph), 57.38 (dd, J_{PC} = 27.0, 15.1 Hz, N*C*(CH$_3$)$_3$), 32.79 (dt, J_{PC} = 39.6, 16.3 Hz, NC(*C*H$_3$)$_3$) 32.48 (t, J_{PC} = 11.9 Hz, NC(*C*H$_3$)$_3$), 31.04 (t, J_{PC} = 6.50 Hz, NC(*C*H$_3$)$_3$), 28.88 (t, J_{PC} = 6.51 Hz, NC(*C*H$_3$)$_3$). ^{31}P{^{1}H} NMR (benzene-d_6, 25 °C): 203.05 (d, J_{PP} = 6.13 Hz), 69.67 (s). Anal. Calcd for $C_{22}H_{41}N_4P_3$: C, 58.14; H, 9.09; N, 12.33. Found: C, 57.84; H, 9.30; N, 12.61.

[(tBuNP)$_2$(tBuN)$_2$]AsPh, 2b

In a manner analogous to that used for the synthesis of **1b, 2a** (1.30 g, 2.85 mmol) in toluene (25 mL) was treated with PhMgCl (1.60 mL, 3.04 mmol). The ensuing light-yellow solution was concentrated *in vacuo* and stored at 12 °C to yield colorless, plate-shaped crystals. Yield: (1.23 g, 2.48 mmol), 87%. Mp: 140–141 °C. ^{1}H NMR (benzene-d_6, 25 °C): 8.36 (d, 2H, *J* = 7.60 Hz, Ph, *ortho*), 7.23 (t, 2H, *J* = 8.00 Hz, Ph, *meta*), 7.04 (t, 1H, *J* = 6.80 Hz, Ph, *para*), 1.46 (s, 9H, N^{t}Bu, amino), 1.39 (s, 9H, N^{t}Bu, imino, N1), 1.33 (s, 18H, N^{t}Bu, imino, N2). ^{13}C{^{1}H} NMR (benzene-d_6, 25 ^{o}C): 152.09 (s, Ph, *ipso*), 133.32 (s, Ph), 129.97 (s, Ph), 57.96 (t, J_{PC} = 9.39 Hz, N*C*(CH$_3$)$_3$), 53.67 (t, J_{PC} = 15.07 Hz, NC(*C*H$_3$)$_3$), 52.05 (t, J_{PC} = 4.89 Hz, NC(*C*H$_3$)$_3$), 32.97 (t, J_{PC} = 5.93 Hz, NC(*C*H$_3$)$_3$), 30.69 (t, J_{PC} = 5.92 Hz, NC(*C*H$_3$)$_3$), 29.72 (t, *J* = 8.24 Hz). ^{31}P{^{1}H} NMR (benzene-d_6, 25 °C): 172.08 (s). Anal. Calcd for $C_{22}H_{41}AsN_4P_2$: C, 53.01; H, 8.29; N, 11.24. Found: C, 52.58; H, 8.01; N, 10.89.

[(tBuNP)$_2$(tBuN)$_2$]SbPh, 3b

To a cooled (0 °C) solution of **3a** (0.58 g, 1.2 mmol) in toluene (20 mL) was added 0.82 mL (1.2 mmol) of PhMgCl dropwise, and the mixture was stirred at rt for 24 h. The $MgCl_2$ was then removed with a frit,

and the ensuing colorless solution was concentrated *in vacuo* and stored at 12 °C. After 24 h, colorless, hexagonal crystals were isolated. Yield: (0.57 g, 1.1 mmol), 91%. Mp: 162–164 °C. ^{1}H NMR (benzene-d_6, 25 °C): 8.21 (d, 2H, J_{HH} = 7.30 Hz, Ph), 7.29 (t, H, J_{HH} = 7.35 Hz, Ph), 7.13 (t, 1 H, J_{HH} = 1.45 Hz, 1.0 Hz, Ph), 1.48 (s, 9H, NC(CH_3)$_3$), 1.45 (s, 9H, NC(CH_3)$_3$), 1.20 (s, 18H, NC(CH_3)$_3$). ^{13}C{^{1}H} NMR (benzene-d_6, 25 °C): 156.4 (s, Ph, *ipso*), 136.2 (s, Ph), 128.7 (s, Ph), 128.3 (s, Ph), 57.27 (d, J_{PC} = 17.0 Hz, N*C*(CH$_3$)$_3$), 53.75 (t, J_{PC} = 13.3 Hz, N*C*(CH$_3$)$_3$), 52.88 (t, J_{PC} = 13.6 Hz, N*C*(CH$_3$)$_3$), 33.63 (d, J_{PC} = 11.4 Hz, NC(*C*H$_3$)$_3$) 30.95 (t, J_{PC} = 7.14 Hz, NC(*C*H$_3$)$_3$), 29.03 (t, J_{PC} = 7.14 Hz, CH$_3$, NC(*C*H$_3$)$_3$). ^{31}P{^{1}H} NMR (benzene-d_6, 25 °C): 138.3 (s). Anal. Calcd for $C_{22}H_{41}N_4P_2Sb$: C, 48.46; H, 7.58; N, 10.27. Found: C, 48.66; H, 7.89; N, 10.10.

{[(^{t}BuNP)$_2$(^{t}BuN)$_2$]BiPh}, 4b

In a manner analogous to that used for the synthesis of **2b**, **4a** (0.93 g, 1.6 mmol) in toluene (25 mL) was treated with PhMgCl (1.17 mL, 1.66 mmol). The ensuing light-yellow solution was concentrated *in vacuo* and stored at –12 °C to yield colorless, needles of **4b**. Yield: (0.89 g, 1.40 mmol), 89%. Mp: 168–170 °C. ^{1}H NMR (benzene-d_6, 25 °C): 8.72 (d, J_{PH} = 7.35 Hz, 2H, Ph, *ortho*), 7.56 (t, J_{PH} = 7.33 Hz, 2H, Ph, *meta*), 7.20 (t, J_{PH} = 8.40, 1H, Ph, *para*), 1.53 (s, 9H, N^{t}Bu, imido), 1.45 (s, 9H, N^{t}Bu, imido), 1.16 (s, 18H, N^{t}Bu, amido). ^{13}C{^{1}H} NMR (benzene-d_6, 25 °C): 139.18 (s, Ph, *ipso*), 135.00 (s, Ph, *ortho*), 132.12 (s, Ph, *meta*), 130.69 (s, Ph, *para*), 56.49 (d, J_{PC} = 17.03 Hz, N*C*(CH$_3$)$_3$, amido), 54.26 (t, J_{PC} = 15.12 Hz, N*C*(CH$_3$)$_3$, imido), 53.28 (t, J_{PC} = 15.50 Hz, N*C*(CH$_3$)$_3$, imido), 34.78 (d, J_{PC} = 11.44 Hz, NC(*C*H$_3$)$_3$, imido), 31.24 (t, J_{PC} = 7.51 Hz, NC(*C*H$_3$)$_3$, imido), 29.99 (t, J_{PC} = 6.44 Hz, NC(*C*H$_3$)$_3$, imido). ^{31}P{^{1}H} NMR (benzene-d_6, 25 °C): 129.67 (s). Anal. Calcd. for $C_{22}H_{41}BiN_4P_2$: C, 41.78; H, 6.53; N, 8.86. Found: C, 41.61; H, 6.35; N, 8.23.

[(^{t}BuNP)$_2$(^{t}BuN)$_2$]PO^{t}Bu, 1e

In a 100-mL two-necked flask **1a** (0.68 g, 1.6 mmol) and NaO^{t}Bu (0.16 g, 1.7 mmol) were mixed in 35 mL of toluene and stirred at 70 °C for 24 h. After the reaction had been allowed to cool to rt, the NaCl was

removed with a frit. The resulting colorless solution was concentrated *in vacuo* to about 10 mL and stored at 12 °C for 3 days. This produced colorless, blocked-shaped crystals. Yield: (0.66 g, 1.46 mmol), 89%. Mp: 186–188 °C. ^{1}H NMR (benzene-d_6, 25 °C): 1.55 (s, 18H, NC(CH_3)$_3$), 1.51 (s, 9H, O^{t}Bu), 1.42 (s, 9H, NC(CH_3)$_3$), 1.39 (s, 9H, NC(CH_3)$_3$). ^{13}C{^{1}H} NMR (benzene-d_6, 25 °C): 76.68 (d, J_{PC} = 15.7 Hz, O*C*(CH$_3$)$_3$), 57.13 (m, N*C*(CH$_3$)$_3$), 53.00 (t, J_{PC} = 7.12 Hz, N*C*(CH$_3$)$_3$), 32.79 (t, J_{PC} = 12.9 Hz, NC(*C*H$_3$)$_3$), 31.81 (d, J_{PC} = 7.27 Hz, OC(*C*H$_3$)$_3$), 30.09 (t, J_{PC} = 6.72 Hz, NC(*C*H$_3$)$_3$), 29.19 (t, J_{PC} = 6.15 Hz, NC(*C*H$_3$)$_3$). ^{31}P{^{1}H} NMR (benzene-d_6, 25 °C): 200.2 (d, *J*pp = 12.9 Hz), 117.8 (t, *J*pp = 12.0 Hz). Anal. Calcd for $C_{20}H_{45}N_4OP_3$: C, 53.32; H, 10.07; N, 12.44. Found: C, 53.07; H, 10.41; N, 12.03.

{[(tBuNP)$_2$(tBuN)$_2$]AsOtBu}, 2e

Samples of **2a** (0.80 g, 1.75 mmol) and NaO^{t}Bu (0.18 g, 1.83 mmol) were dissolved in toluene (30 mL) and stirred at rt for 24 h. The NaCl was removed with a frit, and the filtrate was concentrated *in vacuo* to 5 mL and stored at – 12 °C for 3 days. This produced colorless, block-shaped crystals of **2e**. Yield: (0.66 g, 1.33 mmol), 76%. Mp: 174 –176 °C. ^{1}H NMR (C_6D_6, 25 °C): 1.58 (s, 9H, O^{t}Bu), 1.52 (s, 27H, N^{t}Bu), 1.41 (s, 9H, imido, N^{t}Bu). ^{13}C{^{1}H} NMR (C_6D_6, 25 °C): 75.44 (s, N*C*(CH$_3$)$_3$, O^{t}Bu), 57.77 (t, J_{PC} = 8.99 Hz, N*C*(CH$_3$)$_3$, amido), 53.27 (t, J_{PC} = 13.65 Hz, N*C*(CH$_3$)$_3$, imido), 52.75 (t, J_{PC} = 7.18 Hz, N*C*(CH$_3$)$_3$, imido), 33.60 (t, J_{PC} = 5.53 Hz, NC(*C*H$_3$)$_3$, amido), 33.28 (s, O^{t}Bu), 30.50 (t, J_{PC} = 6.35 Hz, NC(*C*H$_3$)$_3$, imido), 29.95 (t, J_{PC} = 6.08 Hz, NC(*C*H$_3$)$_3$, imido). ^{31}P{^{1}H} NMR (C_6D_6, 25 °C): 183.08 (s). Anal. Calcd. for $C_{20}H_{45}AsN_4OP_2$: C, 48.58; H, 9.17; N, 11.33. Found: C, 48.12; H, 8.68; N, 10.74.

[(tBuNP)$_2$(tBuN)$_2$]SbOtBu, 3e

In a manner entirely analogous to that used for the synthesis of **2e**, **3a** (0.54 g, 1.1 mmol) and NaO^{t}Bu (0.10 g, 1.1 mmol) were allowed to react in toluene. This afforded colorless, blocked-shaped crystals. Yield: (0.46 g, 0.91 mmol), 79%. Mp: 114–116 °C. ^{1}H NMR (benzene-d_6, 25 °C): 1.54 (s, 18H, NC(CH_3)$_3$),

1.49 (s, 9H, OC(CH_3)$_3$), 1.43 (s, 9 H, NC(CH_3)$_3$), 1.41 (s, 9H, OC(CH_3)$_3$). $^{13}C\{^1H\}$ NMR (benzene-d_6, 25 °C): 74.04 (s, O*C*(CH$_3$)$_3$), 56.80 (d, J_{PC} = 15.5 Hz, N*C*(CH$_3$)$_3$), 53.29 (t, J_{PC} = 12.3 Hz, N*C*(CH$_3$)$_3$), 52.61 (t, J_{PC} = 9.21 Hz, N*C*(CH$_3$)$_3$), 34.52 (d, J_{PC} = 13.3 Hz, NC(*C*H$_3$)$_3$), 34.15 (s, CH$_3$, OC(*C*H$_3$)$_3$), 30.98 (t, J_{PC} = 5.97 Hz, NC(*C*H$_3$)$_3$), 27.95 (t, J_{PC} = 7.32 Hz, NC(*C*H$_3$)$_3$). $^{31}P\{^1H\}$ NMR (benzene-d_6, 25 °C): 158.1 (s). Anal. Calcd for $C_{20}H_{45}N_4OP_2Sb$: C, 44.38; H, 8.38; N, 10.35. Found: C, 44.25; H, 8.71; N, 9.90.

{[(^{t}BuNP)$_2$(^{t}BuN)$_2$]AsOPh}, 2f

To a sample of **2a** (1.00 g, 2.19 mmol), dissolved in toluene (10 mL), was added via a syringe a lithium phenoxide solution (1.0 M, 2.30 mL). The pale-yellow reaction mixture was stirred at rt for 1 day, volatiles were removed *in vacuo,* and the residue was extracted with toluene (15 mL). The extract was filtered with a frit, concentrated to 3 mL and stored at –15 °C. Colorless, block-shaped crystals of **2f** were collected after several days. Yield: (0.88 g, 1.71 mmol), 78%. Mp: 113–114 °C. ^1H NMR (benzene-d_6, 25 °C): 7.20 (t, J_{PH} = 7.61 Hz, 2H, *meta*), 7.15 (m, 2H, *ortho*), 6.85 (t, J_{PH} = 7.03 Hz, 1H, *para*), 1.59 (s, 9H, N^{t}Bu, imido), 1.40 (s, 18H, N^{t}Bu, amido), 1.36 (s, 9H, N^{t}Bu, imido). $^{13}C\{^1H\}$ NMR (benzene-d_6, 25 °C): 159.60 (s, Ph, *ipso*), 130.09 (s, Ph, *ortho*), 120.25 (s, Ph, *meta*), 118.72 (s, Ph, *para*), 57.83 (t, J_{PC} = 9.03 Hz, N*C*(CH$_3$)$_3$, amido), 53.09 (t, J_{PC} = 13.13 Hz, N*C*(CH$_3$)$_3$, imido), 52.07 (t, J_{PC} = 5.75 Hz, N*C*(CH$_3$)$_3$, imido), 33.08 (t, J_{PC} = 5.67 Hz, NC(*C*H$_3$)$_3$, amido), 30.09 (t, J_{PC} = 6.34 Hz, NC(*C*H$_3$)$_3$, imido), 29.87 (t, J_{PC} = 6.34 Hz, NC(*C*H$_3$)$_3$, imido). $^{31}P\{^1H\}$ NMR (benzene-d_6, 25 °C): 182.18 (s). Anal. Calcd. for $C_{22}H_{41}AsN_4OP_2$: C, 51.36; H, 8.03; N, 10.89. Found: C, 51.06; H, 8.25; N, 10.39.

{[(^{t}BuNP)$_2$(^{t}BuN)$_2$]AsN$_3$}, 2c

In a 100-mL two-necked flask 0.900 g (1.97 mmol) of **2a** and NaN_3 (0.141 g, 2.17 mmol) were combined in THF (12 mL) and then stirred for 24 h at rt while the light-orange suspension slowly turned cloudy. THF was removed *in vacuo,* and the crystalline residue was extracted with toluene (15 mL). The filtered

extract was concentrated to 3 mL and stored at –15 °C. Colorless plates of **2c** were isolated after several days. Yield: (0.772g, 1.67 mmol) 85%. Mp: 110–111 °C. ^{1}H NMR (benzene-d_6, 21 °C): δ = 1.45 (s, 9H), 1.38 (s, 18H), 1.22 (s, 9H). ^{31}C{^{1}H} NMR (benzene-d_6, 21 °C): δ = 58.04 (t, J = 8.47 Hz), 53.42 (t, J = 13.59 Hz), 51.96 (t, J = 4.70 Hz), 32.59 (t, J = 5.30 Hz), 29.84 (t, J = 7.07 Hz), 29.68 (t, J = 6.10 Hz). ^{31}P{^{1}H} NMR (benzene-d_6, 21 °C): δ = 183.05 (s). Anal. Calcd for $C_{16}H_{36}AsN_7P_2$: C 41.47 H 7.83 N 21.16. Found: 41.15 H 7.76 N 20.18.

{[(^{t}BuNP)$_2$(^{t}BuN)$_2$]AsN(SiMe$_3$)$_2$}, 2d

A cooled (0 °C) THF (8 mL) solution of lithium hexamethyldisilylamide (0.40 g, 2.38 mmol) was treated dropwise with a solution of **2a** (1.00 g, 2.19 mmol) in toluene (24 mL). The reaction mixture which turned orange with the formation of lithium chloride, was stirred for 1 day at rt. All volatiles were removed *in vacuo*, and the residue was extracted with toluene (15 mL). The resulting filtrate was concentrated *in vacuo* to ca. 5 mL and cooled at –6 °C for two days to furnish colorless crystals of **2d**. Yield: (1.15 g, 1.98 mmol), 91%. Mp: 139–140 °C. ^{1}H NMR (C_6D_6, 25 °C): 1.53 (s, 18H, N^{t}Bu, amido), 1.40 (s, 9H, N^{t}Bu, imido), 1.33 (s, 9H, N^{t}Bu, imido), 0.58 (s, 9H, Si(CH$_3$)$_3$), 0.40 (s, 9H, Si(CH$_3$)$_3$). ^{13}C{^{1}H} NMR (C_6D_6, 25 °C): 58.66 (t, J_{PC} = 11.10 Hz, N*C*(CH$_3$)$_3$, amido), 54.34 (t, J_{PC} = 16.98 Hz, N*C*(CH$_3$)$_3$, imido), 52.58 (t, J_{PC} = 7.19 Hz, N*C*(CH$_3$)$_3$, imido), 34.36 (t, J_{PC} = 7.25 Hz, NC(*C*H$_3$)$_3$, amido), 30.85 (t, J_{PC} = 6.11 Hz, NC(*C*H$_3$)$_3$, imido), 29.22 (t, J_{PC} = 9.16 Hz, NC(*C*H$_3$)$_3$, imido), 7.44 (s, Si(CH$_3$)$_3$), 5.61 (s, Si(CH$_3$)$_3$). ^{31}P{^{1}H} NMR (C_6D_6, 25 °C): 186.98 (s). Anal. Calcd. for $C_{22}H_{54}AsN_5P_2Si_2$: C, 45.42; H, 9.36; N, 12.04. Found: C, 45.85; H, 9.65; N, 12.04.

{[(^{t}BuNP)$_2$(^{t}BuN)$_2$]BiN(SiMe$_3$)$_2$}, 4d

Lithium hexamethyldisilylamide **(**0.248 g, 1.48 mmol), dissolved in cold (0 °C) THF (10 mL), was treated dropwise with **4a** (0.874 g, 1.48 mmol) dissolved in toluene (25 mL). The reaction mixture, which turned

orange with the formation of a lithium chloride precipitate, was stirred at rt. All volatiles were removed *in vacuo*, and the residue was extracted with toluene (15 mL). After the filtrate had been stored at –6 °C for 3 days, colorless crystals formed. Yield: (0.825 g, 1.15 mmol) 78%. Mp: 211–212 °C. ^{1}H NMR (benzene-d_6, 21 °C): δ = 1.45 (s, 18H), 1.37 (s, 9H), 1.29 (s, 9H), 0.67 (s, 9H), 0.29 (s, 9H). ^{13}C{^{1}H} NMR (benzene-d_6, 21 °C): δ = 58.08 (d, J = 15.44 Hz), 54.81 (t, J = 14.95 Hz), 54.22 (t, J = 17.13 Hz), 36.24 (d, J = 12.63 Hz), 30.43 (t, J = 9.18 Hz), 28.26 (t, J = 6.83 Hz), 8.25 (s), 5.95 (s,). ^{31}P{^{1}H} NMR (benzene-d_6, 21 °C): δ = 147.89(s). Anal. Calcd for $C_{22}H_{54}AsN_5P_2Si_2$: C 36.92 H 7.60 N 9.78. Found: C 37.02 H 7.64 N 9.52.

[(^{t}BuNP)$_2$(^{t}BuN)$_2$P]$^{+}$ [SO$_3$CF$_3$]$^{-}$, 1g

In a 100 mL flask, a cooled (0 °C) $CHCl_3$ (10 mL) solution of $AgSO_3CF_3$ (0.25 g, 0.97 mmol) was treated dropwise with **1a**, (0.72 g, 1.8 mmol) in $CHCl_3$ (20 mL). A colorless precipitate formed instantly. The reaction mixture was stirred at 0 °C for 30 minutes, and the AgCl was removed with a frit. The ensuing colorless solution, which was concentrated *in vacuo* and stored at 20 °C, deposited colorless, needles after 24 h. Yield: (0.87 g, 1.6 mmol), 90%. Mp: 119–121 °C. ^{1}H NMR (CD_2Cl_2, 25 °C): 1.73 (s, 9H, NC(CH$_3$)$_3$), 1.46 (s, 27H, NC(CH$_3$)$_3$). ^{13}C{^{1}H} NMR (CD_2Cl_2, 25 °C): 119.7 (q, J_{CF} = 319.5 Hz, CF_3), 60.65 (q, J_{PC} = 8.48 Hz, N*C*(CH$_3$)$_3$), 57.23 (t, J_{PC} = 7.82 Hz, N*C*(CH$_3$)$_3$), 31.30 (t, J_{PC} = 5.79 Hz, NC(*C*H$_3$)$_3$), 22.81 (q, J_{PC} = 5.21 Hz, NC(*C*H$_3$)$_3$). ^{31}P{^{1}H} NMR (CD_2Cl_2, 25 °C): 210.4 (s). Anal. Calcd for $C_{17}H_{36}F_3N_4O_3P_3S$: C, 38.78; H, 6.89; N, 10.64. Found: C, 38.63; H, 7.19; N, 10.33.

{[(^{t}BuNP)$_2$(^{t}BuN)$_2$]SbOSO$_2$CF$_3$}, 3g

To a solution of $AgOSO_2CF_3$ (0.28 g, 1.09 mmol) in cold THF (0 °C, 5 ml) was added dropwise a solution of [(^{t}BuNP)$_2$(^{t}BuN)$_2$]SbCl **3a** (0.50 g, 0.99 mmol) in chloroform (10 mL). A white precipitate of AgCl formed instantly. The reaction mixture was stirred at 0 °C for 30 minutes. All volatiles were removed *in*

vacuo, and the residue was extracted with chloroform. The AgCl was removed with a frit, and the ensuing colorless solution was concentrated *in vacuo* and stored at – 20 °C. Colorless, needles of **3g** deposited after 24 h. Yield: (0.56 g, 0.91 mmol), 92%.

Alternatively, **3a** (0.60 g, 1.20 mmol) and $AgOSO_2CF_3$ (0.29 g, 1.10 mmol) were combined in toluene (20 mL), and the mixture was stirred at rt for 1 h. Yield: (0.60 g, 0.97 mmol), 81%. Mp: 156–158 °C. ^{1}H NMR (C_6D_6, 25 °C): 1.46 (s, 18H, N^{t}Bu, amido), 1.10 (s, 18H, N^{t}Bu, imido). ^{13}C{^{1}H} NMR (C_6D_6, 25 °C): 120.1 (q, J_{CF} = 319.0 Hz, CF_3), 57.91 (t, J_{PC} = 5.80 Hz, N*C*$(CH_3)_3$, amido), 54.96 (t, J_{PC} = 10.37 Hz, N*C*$(CH_3)_3$, imido), 33.61 (t, J_{PC} = 6.63 Hz, NC(*C*$H_3)_3$, amido), 27.85 (s, NC(*C*$H_3)_3$, imido).^{31}P{^{1}H} NMR (C_6D_6, 25 °C): 182.73 (s). Anal. Calcd for $C_{17}H_{36}F_3N_4O_3P_2SSb$: C, 33.08; H, 5.88; N, 9.08. Found: C, 32.92; H, 5.93; N, 8.60.

{[(^{t}BuNP)$_2$(^{t}BuN)$_2$]PI}, 1h

Samples of **1a** (0.50 g, 1.21 mmol) and NaI (0.21 g, 1.40 mmol) were combined in THF (20 mL), and the mixture was stirred at rt for 24 h. The mixture was filtered, concentrated *in vacuo*, and stored at – 6 °C to furnish block-shaped, yellow crystals of **1h** after 24 h. Yield: (0.56 g, 1.10 mmol), 91%. Mp: 212–214 °C. ^{1}H NMR ($CDCl_3$, 25 °C): 1.61 (d, J_{PH} = 4.77 Hz), 18H, N^{t}Bu, amido), 1.35 (s, 18H, N^{t}Bu, imido).^{13}C{^{1}H} NMR ($CDCl_3$, 25 °C): 60.84 (m, N*C*$(CH_3)_3$, amido), 53.55 (s, N*C*$(CH_3)_3$, imido), 29.02 (m, NC(*C*$H_3)_3$, imido). ^{31}P{^{1}H} NMR ($CDCl_3$, 25 °C): 196.42 (d, J_{PP} = 28.71 Hz), 173.77 (t, J_{PP} = 27.15 Hz). Anal. Calcd. for $C_{16}H_{36}IN_4P$: C, 38.11; H, 7.19; N, 11.11. Found: C, 37.72; H, 7.27; N, 10.79.

{[(^{t}BuNP)$_2$(^{t}BuN)$_2$]AsI}, 2h

Analogous to the synthesis of **1h, 2a** (0.60 g, 1.3 mmol) and NaI (0.21 g, 1.4 mmol) were stirred in THF (20 mL). The ensuing light-yellow solution was concentrated *in vacuo* and stored at – 6 °C to afford yellow, block-shaped crystals of **2h** after 24 h. Yield: (0.67 g, 1.22 mmol), 93%. Mp: 186–188 °C. ^{1}H NMR

($CDCl_3$, 25 °C): 1.54 (s, 27H, N^{t}Bu) 1.33 (br, 9H, N^{t}Bu, imido). $^{13}C\{^1H\}$ NMR ($CDCl_3$, 25 °C): 60.38 (t, J_{PC} = 8.58 Hz, N*C*$(CH_3)_3$, amido), 53.30 (s, N*C*$(CH_3)_3$, imido), 30.02 (t, J_{PC} = 4.89 Hz, NC(*C*$H_3)_3$, amido), 29.10 (s, NC(*C*$H_3)_3$, imido). $^{31}P\{^1H\}$ NMR ($CDCl_3$, 25 °C): 182.44 (s). Anal. Calcd. for $C_{16}H_{36}AsIN_4P_2$: C, 35.05; H, 6.62; N, 10.22. Found: C, 35.12; H, 6.65; N, 9.96.

{[(^{t}BuNP)$_2$(^{t}BuN)$_2$]SbI}, 3h

A sample of **3a** (0.60 g, 1.2 mmol) and NaI (0.19 g, 1.3 mmol) were stirred in THF (20 mL) at rt for 1 day. The resulting light-yellow mixture was filtered, concentrated *in vacuo,* and stored at – 6 °C to furnish yellow needles of **3h** after 3 days. Yield: (0.62 g, 1.1 mmol), 88%. Mp: 191–193 °C. ^1H NMR ($CDCl_3$, 25 °C): 1.55 (s, 27H, N^{t}Bu), 1.40 (s, 9H, N^{t}Bu). $^{13}C\{^1H\}$ NMR ($CDCl_3$, 25 °C): 59.00 (m, N*C*$(CH_3)_3$), 33.56 (m, NC(*C*$H_3)_3$). $^{31}P\{^1H\}$ NMR ($CDCl_3$, 25 °C): 143.70 (s). Anal. Calcd. for $C_{16}H_{36}IN_4P_2Sb$: C, 32.29; H, 6.10; N, 9.41. Found. C, 31.52; H, 6.28; N, 8.75.

X-ray Crystallography

Crystals of **2b, 3b, 4d, 2c, 1g, 3g** were coated with Paratone oil, affixed to Mitegen or Litholoop crystal holders, and centered on the diffractometer in a stream of cold nitrogen. Reflection intensities were collected with a Bruker Apex diffractometer, equipped with an Oxford Cryosystems, 700 Series Cryostream cooler, operating at 173 K. Data were measured using ω scans of 0.3° per frame for 20 seconds until a complete hemisphere or sphere of data had been collected. Cell parameters were retrieved using SMART[64] software and refined with SAINT[65] on all observed reflections. Data were reduced with SAINTplus, which corrects for Lorentz polarization effects and crystal decay. Empirical absorption corrections were applied with SADABS.[66] The structures were solved by direct methods with

SHELXS-90[67] program and refined by full-matrix least squares methods on F^2 with SHELXL-97 incorporated in SHELXTL Version 5.10.[68]

Crystals of **(1ab)$_2$, 1h, 2h,** and **3h** were coated with Paratone oil, affixed to Mitegen or Litholoop crystal holders and quickly transferred to the goniometer head of a Bruker Quest diffractometer equipped with a fixed χ angle, a sealed fine-focus X-ray tube, a single-crystal curved graphite incident beam monochromator, a Photon100 CMOS area detector and an Oxford Cryosystems low temperature device. Examination and data collection were performed with Mo Kα radiation (λ = 0.71073 Å) at 150 K. Data were collected, reflections were indexed and processed, and the files were scaled and corrected for absorption using APEX3.[69] The space groups were assigned and the structures were solved by direct methods using XPREP within SHELXTL suite programs[70] and refined by full matrix least squares against F^2 with all reflections using Shelxl2018[71] using the graphical interface Shelxle.[72] If not specified otherwise H atoms attached to carbon and nitrogen atoms were positioned geometrically and constrained to ride on their parent atoms. C–H bond distances were constrained to 0.95 Å for aromatic and CH_2 moieties, and to 1.00, 0.99 and 0.98 Å for aliphatic CH, CH_2 and CH_3 moieties, respectively. Methyl groups were allowed to rotate but not to tip to best fit the experimental electron density. CCDC 1960508, 1991877, 1991878, 1991882–1991887, 1991892 contain the supplementary crystallographic data for this paper. These data can be obtained free of charge from The Cambridge Crystallographic Data Centre via www.ccdc.cam.ac.uk/data_request/cif.

Conflicts of interest

There are no conflicts of interest to declare.

Acknowledgments

This material is based in part upon work carried out at the X-ray facility in the Chemistry Department of Purdue University, which is supported by the National Science Foundation through the Major Research Instrumentation Program under Grant No. CHE 1625543.

References

1 R. R. Holmes and J. A. Forstner, *Inorg. Chem.* 1963, **2**, 380–384.

2 O. J. Scherer and P. Klusmann, *Angew. Chem. Int. Ed.,* 1969, **8**, 752–753.

3 K. W. Muir and J. F. Nixon, *J. Chem. Soc., Chem. Comm.,* 1971, 1405–1406.

4 K. W. Muir, *J. Chem. Soc., Dalton Trans.,* 1975, 259–262.

5 E. Niecke, W. Flick and S. Pohl, *Angew. Chem. Int. Ed. Eng.,* 1976, **15**, 309–310.

6 O. J. Scherer, G. Wolmershäuser and H. Conrad, *Angew. Chem. Int. Ed.,* 1983, **22**, 404–405.

7 S. S. Kumaravel, S. S. Krishnamurthy, T. S. Cameron and A. Linden, *Inorg. Chem.,* 1988, 27, 4546–4550.

8 D. Linti, H. Nöth, E. Schneider and W. Storch, *Chem. Ber.,* 1993, **126**, 619–626.

9 M. S. Balakrishna, R. Venkateswaran and J. T. Mague, *Inorg. Chem*., 2009, **48**, 1398–1406.

10 P. Chandrasekaran, J. T. Mague and M. S. Balakrishna, *Dalton Trans*., 2009, 5478–5486.

11 P. Chandrasekaran, J. T. Mague and M. S. Balakrishna, *Inorg. Chem*., 2005, **44**, 7925–7932.

12 D. Suresh, M. S. Balakrishna and J. T. Mague, *Dalton Trans*., 2008, 3272–3274.

13 P. Chandrasekaran, J. T. Mague and M. S. Balakrishna, *Organometallics*, 2005, **24**, 3780–3783.

14 G. S. Ananthnag, S. Kuntavalli, J. T. Mague and M. S. Balakrishna, *Inorg. Chem.*, 2012, **51**, 5919–5930.

15 P. Chandrasekaran, J. T. Mague and M. S. Balakrishna, *Dalton Trans.*, 2007, 2957–2962.

16 M. S. Balakrishna, V. S. Reddy, S. S. Krishnamurthy, J. F. Nixon and J. C. T. R. Burckett, *Coord. Chem. Rev.* 1994, **129**, 1–90.

17 L. Grocholl, V. Huch, L. Stahl, R. J. Staples, P. Steinhart and A. Johnson, *Inorg. Chem.,* 1997, **36**, 4451–4457.

18 L. Grocholl, L. Stahl and R. J. Staples, *Chem. Commun.,* 1997, 1465–1466.

19 I. Schranz, L. Stahl and R. J. Staples, *Inorg. Chem.,* 1998, **37**, 1493–1498.

20 M. Otang, G. R. Lief and L. Stahl, *J. Organomet. Chem.,* 2016, **820**, 98–110.

21 D. F. Moser, I. Schranz, M. C. Gerrety, L. Stahl and R. J. Staples, *J. Chem. Soc., Dalton Trans.,* 1999, 751–757.

22 D. F. Moser, C. J. Carrow, L. Stahl and R. J. Staples, *J. Chem. Soc., Dalton Trans.* 2001, 1246–1252.

23 D. F. Moser, L. Grocholl, L. Stahl and R. J. Staples, *Dalton Trans.,* 2003, 1402–1410.

24 I. Schranz, L. P. Grocholl, L. Stahl, R. J. Staples and A. Johnson, *Inorg. Chem.,* 2000, **39**, 3037–3041.

25 M. E. Otang, D. Josephson, T. Duppong and L. Stahl, *Dalton Trans.,* 2018, **47**, 11625–11635.

26 N. Burford and D. J. LeBlanc, *Inorg. Chem.* 1999, **38,** 2248–2249.

27 M. Rastätter, P. W. Roesky, D. Gudat, G. B. Deacon and P. C. Junk, *Chem. Eur. J.* 2007, **13**, 7410–7415.

28 K. V. Axenov, M. Klinga, M. Leskelä, V. Kotov and T. Repo, *Eur. J. Inorg. Chem., 2004*, 4702–4709.

29 K. V. Axenov, M. Klinga, M. Leskelä and T. Repo, *Organometallics,* 2005, **24**, 1336–1343.

30 T. G. Hill, R. C. Haltiwanger, M. L. Thompson, S. A. Katz and A. D. Norman, *Inorg. Chem.,* 1994, **33**, 1770–1777.

31 T. G. Hill, R. C. Haltiwanger, T. R. Prout and A. D. Norman, *Inorg. Chem.,* 1989, **33**, 3461–3467.

32 F. Garcia, J. M. Goodman, R. A. Kowenicki, M. McPartlin, L. Riera, M. A. Silva, A. Wirsing and D. S. Wright, *Dalton Trans.,* 2005, 1764–1773.

33 S. G. Calera and D. S. Wright, *Dalton Trans.,* 2010, **39**, 5055–5065.

34 H.-C. Niu, A. J. Plajer, R. Garcia-Rodriquez, S. Singh and D. S. Wright, *Chem. Eur. J.,* 2018, **24**, 3073–3082.

35 Y. X. Shi, R. Z. Liang, K. A. Martin, D. G. Star, J. Díaz, X. Y. Li, R. Ganguly and F. García, *Chem. Commun.* 2015, **51**, 16468–16471.

36 Y. X. Shi, K. A. Martin, R. Z. Liang, D. G. Star, Y. Li, R. Ganguly, Y. Sim, D. Tan, J. Díaz and F. García, *Inorg. Chem.* 2018, **57**, 10993–11004.

37 J. K. Brask, T. Chivers, M. L. Krahn and M. Parvez, *Inorg. Chem.,* 1999, **38**, 290–295.

38 T. Chivers, M. Krahn, M. Parvez and G. Schatte, *Inorg. Chem.,* 2001, **40**, 2547–2553.

39 T. Chivers, M. Krahn and M. Parvez, *Chem. Commun.,* 2000, 463–464.

40 T. Chivers, C. Fedorchuk, M. Krahn, M. Parvez and G. Schatte, *Inorg. Chem.,* 2001, **40**, 1936–1942.

41 G. G. Briand, T. Chivers and G. Schatte, *Inorg. Chem.,* 2002, **41**, 1958–1965.

42 A. Nordheider, T. Chivers, R. Thirumoorthi, I. Vargas-Baca and J. D. Woollins, *Chem. Commun.,* 2012, **48**, 6346–6348.

43 A. Nordheider, T. Chivers, R. Thirumoorthi, K. S. A. Arachchige, A. M. Z. Slawin, J. D. Woollins and I. Vargas-Baca, *Dalton Trans.,* 2013, **42**, 3291–3294.

44 A. Hinz, A. Schulz, A. Villinger and N. Weding, *Chem. Eur. J.*, 2014, **20**, 3913–3916.

45 A. Hinz, J. Rothe, A. Schulz, A. Villinger, *Dalton Trans.*, 2016, **45**, 6044-6052.

46 L. Stahl, *Coord. Chem. Rev.,* 2000, **210**, 203–250.

47 J. K. Brask and T. Chivers, *Angew. Chem. Int. Ed.* 2001, **40**, 3960–3976.

48 G. G. Briand, T. Chivers and M. Krahn, *Coord. Chem. Rev.* 2002**, 233–234**, 237–254.

49 M. S.Balakrishna, D. J. Eisler and T. Chivers, *Chem. Soc. Rev.* 2007, **36**, 650–664.

50 M. S. Balakrishna, *Dalton Trans.* 2016, **45**, 12252–12282.

51 R. Haiges, A. Vij, J. A. Boatz, S. Schneider, T. Schroer, M. Gerken and K. O. Christe, *Chem. Eur. J.* 2004, **10**, 508–517.

52 R. Haiges, M. Rahm, D. A. Dixon, E. B. Garner, III, and K. O. Christe, *Inorg. Chem.*, 2011, **51**, 1127–1141.

53 G. E. Pringle and D. E. Noakes, *Acta Cryst. B.*, 1968, **24,** 262–269**.**

54 D. Winkelhaus, M. H. Holthausen, R. Dobrovetsky and D. W. Stephan, *Chem. Sci.,* 2015, **6**, 6367–6372.

55 D. Michalik, A. Schulz, A. Villinger and N. Weding, *Angew. Chem. Int. Ed.*, 2008, **47**, 6465–6468.

56 B. Cordero, V. Gómez, A. E. Platero-Prats, Marc Revès, J. Echeverría, E. Cremades, F. Barragan and S. Alvarez. *Dalton Trans.,* **2008**, 2832–2838.

57 M. Gonsior, I. Krossing, L. Müller, I. Raabe, M. Jansen and L. van Wüllen, *Chem. Eur. J.*, 2002, **8**, 4475–4492.

58 I. Krossing and I. Raabe, *Angew. Chem. Int. Ed.*, 2001, **40**, 4406–4409.

59 H.A. Spinney, I. Korobkov, G. A. DiLabio, G. P. A. Yap and D. S. Richeson, *Organometallics*, 2007, **26**, 4972–4982.

60 A. P. M. Robertson, P. A. Gray and N. Burford, *Angew. Chem. Int. Ed.,* 2014, **53**, 6050–6069.

61 S. S. Chitnis, A. P. M. Robertson, N. Burford, B. O. Patrick, R. McDonald and M. J. Ferguson, *Chem. Sci.* 2015, **6**, 6545–6555.

62 Y.-J. Carpenter, N. Burford, M. D. Lumsden and R. McDonald, *Inorg. Chem.* 2011, **50**, 3342–3353.

63 C. Hering, J. Rothe, A. Schulz and A. Villinger, *Inorg. Chem.*, 2013, **52**, 7781–7790.

64 SMART Version 4.053, Siemens Analytical X-ray Systems. Madison, WI, 1995.

65 SAINT Version 4.035, Siemens Analytical X-ray Systems. Madison, WI, 1995.

66 SADABS Program for Absorption Corrections Using the Bruker CCD Detector System. Based on: Blessing, R. H. *Acta Cryst.,* 1995, A51, 33–38.

67 G. M. Sheldrick, SHELXS-90, Program for the Solution of Crystal Structures. University of Göttingen, Göttingen, Germany, **1990**.

68 SHELXTL 5.10 (PC-Version), Siemens Analytical X-Ray Instruments, Inc. Madison, WI, **1998**.

69 Bruker, Apex3 V 2016.9-0, Saint V8.34A, SAINTV8.37A, Bruker AXS Inc. Madison, WI, USA, **2016**.

70 SHELXTL, Suite of programs, Version 6.14, Bruker Advanced X-ray Solutions, Bruker AXS Inc., Madison, WI, USA, **2000–2003**.

71 G. M. Sheldrick, Crystal Structure Refinement with SHELXL. *Acta Cryst. C.* 2015, **71**, 3–8.

72 C. B Hübschle, G. M. Sheldrick, B. Dittrich, ShelXle: A Qt Graphical User Interface for SHELXL. *J. Appl. Crystallogr.* 2011, **44**, 1281–1284.

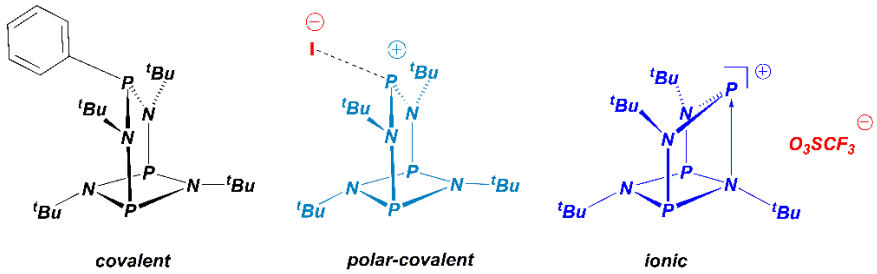

Bonding variations from completely covalent, via polar covalent to completely ionic in bi- and tri-cyclic Group 15 amides.